POLITECNICO
MILANO 1863

DIPARTIMENTO DI MECCANICA

mecc

# Cross-level model of a transfer machine energy demand using a two-machine generalized threshold representation

Wójcicki, Jeremi; Tolio, Tullio; Bianchi, Giacomo

This is a post-peer-review, pre-copyedit version of an article published in JOURNAL OF MANUFACTURING SYSTEMS. The final authenticated version is available online at: http://dx.doi.org/10.1016/j.jmsy.2020.11.011

This content is provided under CC BY-NC-ND 4.0 license

DIPARTIMENTO DI MECCANICA ■ POLITECNICO DI MILANO
via G. La Masa, 1 ■ 20156 Milano ■ EMAIL (PEC): pecmecc@cert.polimi.it
http://www.mecc.polimi.it
Rev. 0

# Cross-level model of a transfer machine energy demand using a two-machine generalized threshold representation

**Jeremi Wójcicki[a]*, Tullio Tolio[b], Giacomo Bianchi[a]**

[a] *CNR-STIIMA, Institute of Intelligent Industrial Technologies and Systems for Advanced Manufacturing, Italian National Research Council*
*Via Alfonso Corti 12, 20133, Milano, Italy*

[b] *Politecnico di Milano, Department of Mechanical Engineering, Via la Masa, 1, 20156 Milan, Italy*

*Corresponding author. E-mail: jeremi.wojcicki@stiima.cnr.it

Keywords: sustainable manufacturing; energy; efficiency; consumption; optimization; machine tools

## Abstract

The paper proposes an energy consumption cross-level model for a demand driven machine tool working in a manufacturing system. The aim is to optimize performance of manufacturing system engaging more than one organizational level, in this case the machine and the system levels. The paper exploits a former study on Pareto optimal Minimum Energy-Time functions, representing the best possible machine setups under varying cycle-time. The functions are used to model machine productive states, whereas stochastic behaviours (failures, blocking, starvation) and inter-machine interactions are described using a Markovian General Threshold Model. Here, instead of using a constant power per machine state assumption, a functional relationship between processing rate and machine energy demand is used. A stand-by energy-saving policy, which exploits the flexibility in adopting a variable processing rate and a settable threshold level of the interoperational parts buffer as a trigger, is developed and benchmarked. The model is used to analyse an industrial case study of a three-station transfer machine. It takes into account a number of cost contributing factors, apart from sole energy demand, such as tooling cost, operator cost, inventory and costs related to potentially undelivered throughput. The application of the proposed cross-level optimization scheme to a case study showed

an improvement both in energy-efficiency and in profitability of the production system under investigation. Moreover, it has been demonstrated that a model exploiting knowledge from both levels can avoid suboptimal setups resulting from treating single-level problems independently.

# 1 Introduction

Optimal setup of a manufacturing system composed of several machines is a non-trivial task. Performance is composed by several factors, among them productivity, quality, cost, but also environmental factors, such as energy demand (Diaz C. and Ocampo-Martinez, 2019). In recent years, research community developed methods for finding optimum work-point of a single processing unit, by adjusting process parameters, rearranging feature processing order or optimizing toolpath (Diaz C. et al., 2020), in an *a priori* optimization/simulation (Mawson and Hughes, 2019) or in real-time at the shop floor level (Hu et al., 2020) . At manufacturing system level, the scope is primarily optimal resource and buffer allocation, including energy-aware job dispatching strategies (Chou et al., 2020), or energy saving policies for machines shutdown (Frigerio and Matta, 2014). However, in a typical scenario, these optimization measures are applied sequentially, without any interaction between machine and system levels. Intuitively, this may lead to suboptimal solutions when, for example, a non-bottleneck machine may be pushed to maximum productivity at the expense of higher tool wear and lower energy efficiency. On the contrary, a tool saving, less aggressive processing strategy might be applied to a machine that is in fact a bottleneck in the production line, hence leading to, respectively, increased costs or reduced productivity of the whole line. Taking a suboptimal decisions in the presented examples leads to a tangible financial consequences of globally suboptimal setup of the whole system, and presents a relevant challenge for industrial manufacturing companies.

This paper addresses this problem by establishing an interaction between machine and system organizational levels at the optimization phase, eliminating the described sub-optimal decisions. The traditional sequential approach is transformed in a hierarchical optimization. Each machining cycle is described as a Pareto-optimal set of energy per part – cycle time pairs, which represent a range of

locally optimal setups for the machine, from the point of view of energy demand and processing rate. This work is a continuation of a study by (Wójcicki et al., 2018a), which focused on the derivation of machine level Pareto front for a single processing unit in isolation, for a given job. In this paper we introduce the inter-level link, demonstrating it on a two machines system, proposing an energy saving policy. The implementation exploits a Markovian Generalized Threshold Model, which models stochastic behaviour of machines by exponentially distributed down-states and realizes control policies based on the actual level of the interoperational buffer. We extend this model to evaluate machines energy demand and compute other cost factors, like tool life, operator wage, throughput loss and inventory cost. An actual industrial case study has been modelled, showing that the proposed approach brings a noticeable benefit in terms of overall cost, compared both to the actual production and to the sequential optimization proposed by the state of the art.

The paper is organized as follows: section 2 contains relevant literature review at machine and system level, section 3 defines the problem of sequential and joint machine and system level optimization. Section 4 introduces the modeling approach for processing rate, energy demand and cost estimation. Section 5 presents the examined industrial case study, whereas section 6 discusses obtained results and critically evaluates the developed method. Section 7 draws the overall conclusions. List of used symbols can be found in Appendix A, whereas the framework for machine state modelling is given in Appendix B.

# 2 Literature review

To improve the efficiency of a manufacturing system, a multitude of factors, like production rate, inventory, operator cost, tooling cost, must be well balanced. In the last decade, a growing attention has being paid to another cost and environmental factor: energy consumption. Actions to reduce manufacturing energy footprint are being deployed at several organizational levels: device/processing unit/machine, line/cell/multi-machine system, facility/factory, multi-factory system (Zhou et al., 2016). This section presents a review of scientific contributions to energy modelling of a manufacturing

process, performed by a machine tool, from a system perspective. The focus is on factors related to part flow, reliability and interaction with other machines through part supply and demand. Two main directions of research are distinguishable: *stochastic discrete-event models*, typically extending on *Markov-chain* representation of state transitions and *hybrid models* attempting to combine information from system and machine levels (or more) to support efficient and energy-saving oriented, process planning or control.

## 2.1 Discrete-event models

A common approach in modelling machines at system level is using discrete-event models, in which a Machine Tool (MT) is represented by means of a state machine diagram, with a different given power consumption for every machine state. While a constant power assumption is a good approximation for non-processing states, during machining, power consumption varies and can strongly depend on selected processing parameters, such as material removal rate (MRR), feed or depth of cut (Wójcicki et al., 2018b). Given the probability distribution of switching from one state to another, one can derive the average energy consumption of a MT or the entire system. Such analysis can focus on a production cell (Dietmair and Verl, 2009; Wang et al., 2013) or on a multi-machine transfer line (Frigerio et al., 2013). This group of methods describes quantities such as supply and demand of parts (representing the interaction with other machines in the line), machine failures, quality control rejection or energy efficiency policies in a probabilistic manner. Formalizing a framework to model system-wide policies for machine stand-by, part handling and inventory management (Gebennini and Grassi, 2015; Levantesi et al., 2003; Tolio and Ratti, 2013a) brings improvements and new possibilities for managing energy efficiency in complex manufacturing systems.

A common system level approach is to find control policies for a machine tool in a production line which minimize base machine consumption, that often contributes to more than half of overall machine consumption. Strategies include putting a machine in a low-energy state (stand-by) when idle, often connected to appropriate part buffers allocation to damp surges in demand, preventing frequent switch-

offs and warm-ups. Mouzon (2007) examined through numerical computation several dispatching strategies, which minimize non-bottleneck machine idle time and reduce number of machine switch-off-on cycles. In the model, parts arrival times were randomly distributed and for energy consumption, a fixed power per state was considered. The study of Prabhu et al. (2012) extended a conventional single server model for a MT by implementing an energy saving policy (Prabhu et al., 2013), which aimed at switching to low energy state when idle time exceeds a settable threshold. Analytical solution to the problem was found making it applicable for decomposition and modelling of long production lines. Another model (Chang et al., 2013) used a numerical simulation to describe dynamics of an automotive manufacturing line, with finite capacity interoperational buffers. It allowed pinpointing energy saving opportunities, defined as periods in which a given machine can be turned off without causing throughput loss. Both presented approaches considered that machines had an energy saving state, which can be activated when idling, with a constant power demand associated with each state. Similar assumption for power demand of a MT was considered Frigerio et al. (2013) who using a Markov-chain "automata"-based approach to define an optimum switch-off strategy, knowing only part-arrival distribution, but not knowing the state of remaining machines. Other implemented policies, relying on time of last parts departure/arrival (Frigerio and Matta, 2014), used the same assumption: constant power demand per state. Similar assumption was used by Zavanella et al. (2015), who applied queueing theory to realize a switch-on model of a machine in an industrial manufacturing system. Finally, a general-threshold model was introduced (Tolio and Ratti, 2018) to evaluate performance of a two machine building block with an interoperational buffer and multiple up and down states. The discrete state, continuous time Markov-chain-based model uses a continuous material flow assumption, which prevents problem explosion for large buffers. It aims at modelling of systems whose behaviour changes depending on the buffer level, and therefore can potentially be used to represent various energy policies.

## 2.2 Hybrid models

The potential benefits of going beyond single-level analysis in a particular production scenarios may be substantial (Peng and Xu, 2014). So far, however, relatively few publications mentioned concepts of hybrid models, which can combine multiple level analysis. A feature-based, cross-level approach was proposed (Peng and Xu, 2013), yet the scope did not fully embrace a multi-machine production scenario. IEC 61499 standard introduced Function Blocks, which represent a variety of models: machine components, machine states or state transition diagrams (Peng et al., 2014). They can form a hierarchy to model a complex manufacturing system energy demand with user-defined resolution. Another work was devoted to an on-line optimization of energy consumption (Verl et al., 2011) by real-time hierarchical optimization loops. Information on energy consumption characteristics of the machine and its components are used in local optimization loops, whose role is to switch controlled components into the lowest possible energy state that meets system requirements.

State of the art analysis shows that combining knowledge from multiple levels (machine, system) has not been fully investigated yet, highlighting as the proposed work can contribute to the knowledge of the field.

# 3 Problem definition

Modern manufacturing systems can be very complex: analysing a machine tool in that context greatly differs from what it would be for a machine in isolation. This is mostly due to system size but also stochasticity coming from unpredictable part demand variation and other sources of randomness, such as machines failures, operator availability etc. Proper buffer allocation, that ensures desired throughput and minimal energy consumption, is a difficult task and has been widely studied (Demir et al., 2014). The literature review shows that most works focus on a single level of analysis, whereas a cross-level approach has been identified as a promising research direction.

System-level energy models typically use a constant power per state assumption. Numerous machine-level studies showed the contrary: the energy per part (and cycle time) depends strongly on the processing parameters. Rief et al. (2017) developed an analytical parametrized model to predict energy demand of a milling cycle, whereas Kant and Sangwan (2015) trained an artificial neural network for the same purpose. These works show a clear relation between used technological parameters and cycle time and energy use. Similar conclusions can be drawn from the literature on power demand of turning operations (Wójcicki et al., 2018b). As scientific studies typically concern one level of analysis, the attempt to optimize a system globally, starting at a machine level (where the machining process is executed) and then using the obtained work-point in a system optimization, inherently brings to a globally suboptimal solution, because of the unresolved coupling between levels. For example, using a minimum energy per part work point (optimal cycle) of a single machine considered in isolation, may adversely affect the system performance, because it does not consider the required production rate or the saturation level of the other machines in the system. Alternatively, a joint multi-level optimization could be performed, resolving cross-level dependencies; however, it could be cumbersome, because of the huge problem size, number of parameters and constraints and, generally, different nature of the two problems.

To tackle the multi-level approach, the authors propose to decouple the two problems, while maintaining an inter-level link, which preserves global optimality: the execution of the process on a specific machine tool is represented by a Pareto-optimal front. It reproduces the Minimum Energy-Time function (MET function), which, in a compact form, retains the outcomes of machine level process optimization. This article relies on the work conducted by Wójcicki et al. (2018a), introducing a framework for machine level modelling during system-level optimization.

This article considers a portion of such system: a demand driven machine tools with a downstream buffer. It is modelled using a two machines system with an inter-operational parts buffer, in literature often defined as a *building block* (Colledani and Tolio, 2005). The role of the second machine is to represent implicitly the demand for parts with a certain probability distribution. The primary function of

the buffer is to stabilize the part flow in case of an unforeseen events, e.g. when one of the machines is temporarily down, thus preventing blocking upstream or starvation downstream. This model is suitable for several industrial cases: a transfer line, a stand-alone, small manufacturing system, flexible manufacturing system or parts of bigger and complex systems with parallel branches.

To evaluate performance of the designed system, typically a steady-state probability of all system states must be found. In this way, the mean throughput and the mean inventory residing in each buffer can be computed. Similarly, if a common approach to assume a fixed power consumption per state of a machine is used, total energy demand per unit of time or per part can be easily estimated.

Markovian processes are often employed to model manufacturing systems, and a continuous time, discrete state convention is typically used for representation of discrete manufacturing systems. Solving Markovian model yields desired steady-state probabilities. One variation of such models is a Generalized Threshold Model (GTM), which can include both random and deterministic transitions between states. Reaching a defined buffer level triggers the transitions. This property is exploited, in this work, to model various machine energy-saving policies, e.g. depending on the buffer level, switching off the machine or putting it in a low-power stand-by mode.

In this scope, the objective is to find an optimal working condition for a machine (further on referred to as *upstream machine*) that interacts with a manufacturing system via supply and demand for parts. Throughput, energy demand, reliability, and inventory are evaluated with the final goal of minimizing the net present cost per part (Fig. 1). The objective function includes the following components: energy bill, inventory, tooling and throughput cost.

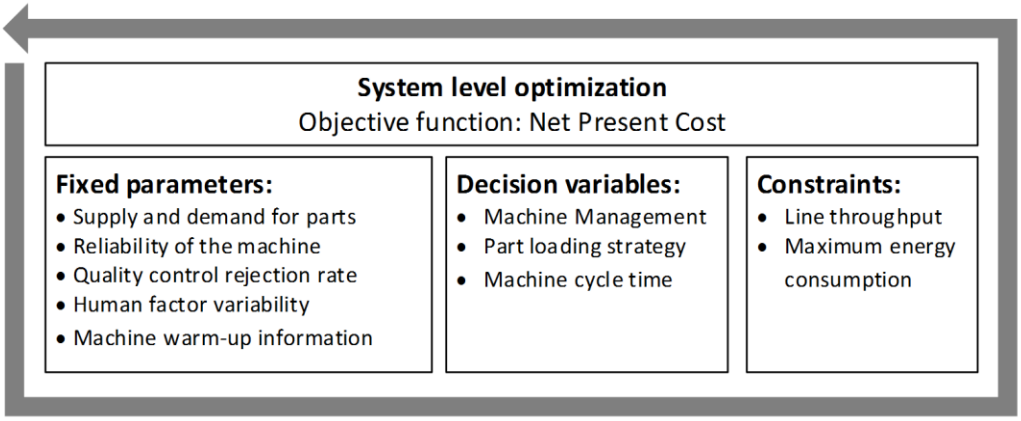


Fig. 1. Graphical representation of machine configuration problem for a given production mission (Wójcicki and Bianchi, 2015).

The considered decision variables are:

a) Machine management: energy saving stand-by policy

b) Cycle time: working point on the MET function

A possible machine management policy is to shut down a MT when it is not used. This simple technique proved to be effective, however decision on when to shut down is not trivial (Weinert and Mose, 2014). Transition from *stand-by* mode to *operational* state (further on referred to as $UP$ state), called *warm-up*, usually needs a certain amount of time and energy, typically to bring the machine into a proper thermal state. Therefore, if the machine would switch to stand-by every time it finishes a single part, it would certainly loose both throughput and energy. Instead, parts may be produced in batches and accumulated in a buffer (either upstream or downstream). Management policy control would trigger the production for a period of time, improving overall efficiency.

Another strategy is to modify machine cycle time, which affects system throughput, inventory and energy per part. The goal of this paper is to describe how a MET function, which relates variable cycle time with energy consumption, can be interfaced to an existing method for manufacturing system evaluation and how changing production rate affects system performance, energy demand included. For example, choosing the fastest machining cycle guarantees the highest throughput, but a slower cycle might be more energy-efficient and less tool-consuming.

# 4 Methodology

## 4.1 Linking machine and system level energy information

Wójcicki and Bianchi (2015) introduced the concept of Minimal Energy-Time function (*MET*), which describes the relation between time and minimum energy to manufacture a part in a MT in isolation. This approach was formalized (Wójcicki et al., 2018a) for the machine level side, using a hierarchical tree of MET functions for all major tasks executed by a machine tool. The final, top-level, function is a compact, Pareto-optimal, representation of the relationship between machining cycle-time and minimum energy-per-part for a MT in isolation. It embeds the knowledge from lower level energy models: subsystems, operations, technological processes and processing stations. In other words, entering with a given cycle-time value on the MET, immediately gives the optimal energy-per-part, considering all machine-level decisions, together with the corresponding vector of process parameters that should be set on the machine. The objective of this work is to propagate knowledge from the machine level compact representation into system level analysis, allowing the use of variable processing rate and corresponding variable energy-per-part representation of the UP state. Compared to the traditional approach, an additional design variable is added to the system optimization problem. The final power absorption in the UP state is then given as a sum of the operation-dependent *MET* function and machine non-productive basal component $P_{base}$:

$$P_{UP}(\mu) = MET\left(\frac{1}{\mu}\right) \cdot \frac{1}{\mu} + P_{base} \tag{1}$$

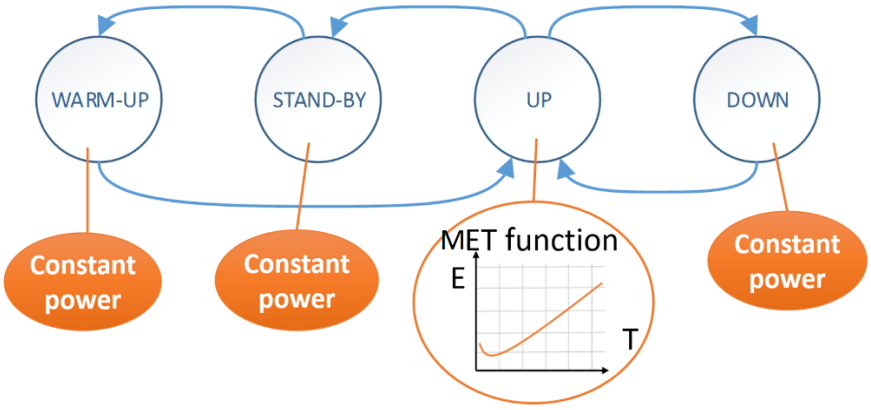


Fig. 2. Example of a discrete-event model of a machine tool with constant power demand associated to each state. Exception is the UP (processing) state, which power demand is given by an MET function, derived in machine level energy analysis (Wójcicki, 2017)

## 4.2 A two machines demand driven system

Two machines linked with an interoperational buffer compose the considered building block. The management policy for the upstream machine is under investigation and its production rate in the *UP* state is settable. The downstream machine simulates a randomly distributed demand for parts, realized through exponentially distributed down states. For the second machine, we consider one UP and two non-producing states: DOWN and SETUP. Its nominal processing rate is constant and is assumed to be less than that one of the upstream machine. This paper considers two variants – a system with or without a stand-by policy. The analysis considers the performance of the upstream machine tool, the sizing of the part buffer and the related control policies. Costs related to the downstream machine is considered as constant and omitted from the optimization.

A *generalized threshold model* (GTM) has been chosen to model the behaviour of a machine in a manufacturing cell, which allows to evaluate the steady state performance a two-machine system with finite buffer implementing stochastic state transition and deterministic policies activated by reaching specified buffer fill levels (thresholds). This section provides an overall description of the approach. Additional information on the model is given in Appendix B, whereas the method of solving a GTM is described in details in (Tolio and Ratti, 2018), and will not be discussed here.

### 4.2.1 System without a stand-by policy

In this variant, the upstream machine continues to operate at given rate (in the range of the MET function), regardless of the buffer level. No stand-by state is defined. When the buffer fills up, the upstream machine is blocked, until at least one slot in the buffer is freed by the demand of the downstream stage. Without specific policies, the machine would produce another part taking that space and blocking itself again. The production would interruptedly continue in this throttling-like manner. Using the continuous part flow assumption of *GTM*, such effect is described as an apparent processing rate reduction, matching the downstream rate. Additionally, at any moment, both upstream and downstream machines can go into down state (respectively with failure rate $\lambda_{dn,u}$ and $\lambda_{dn,d}$) or setup ($\lambda_{ch,u}$ and $\lambda_{ch,d}$). The rate $\lambda_{ch}$ indicates how often production changes, requiring a setup: changing the toolset and the part program, to produce a different part type. Machines recover from these states going back to operational (*UP*) with rates equal to $\lambda_{up,u}$, $\lambda_{up,d}$, $\lambda_{su,u}$, $\lambda_{su,d}$, respectively. The system behaviour is depicted in Fig. 3.

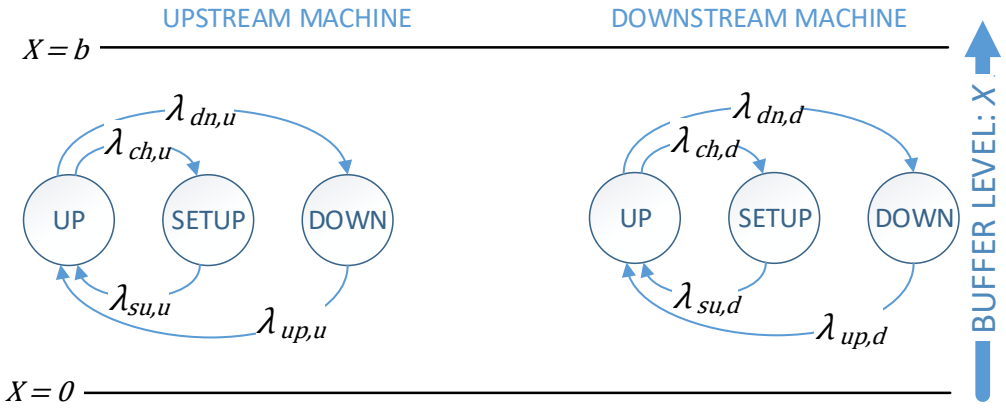


Fig. 3. GTM model diagram for a system with continuous production regime (no stand-by).

For a system with a uniform behaviour, independent from the buffer level (it changes only on its boundaries), *GTM* defines a single buffer range:

$$X_1 = [0, b] \tag{2}$$

States of upstream and downstream machines are simply *UP*, *DOWN* or *SETUP*:

$$S_1^d = S_1^u = [UP, DN, SU] \tag{3}$$

The internal states $\bar{\mu}$ rates for the upstream and the downstream machine are then defined as follows:

$$Q_1^{*\,u} = \begin{bmatrix} 0 & \lambda_{dn,u} & \lambda_{ch,u} \\ \lambda_{up,u} & 0 & 0 \\ \lambda_{su,u} & 0 & 0 \end{bmatrix}$$
$$Q_1^{*\,d} = \begin{bmatrix} 0 & \lambda_{dn,d} & \lambda_{ch,d} \\ \lambda_{up,d} & 0 & 0 \\ \lambda_{su,d} & 0 & 0 \end{bmatrix} \tag{4}$$

No state change (*control policy*) occurs at the boundaries, so a one-to-one mapping describes the on-threshold behaviour:

$$Z_1^{u-} = Z_1^{u+} = Z_1^{d-} = Z_1^{d+} = [1\ 1\ 1]$$
$$Y_1^{u-} = Y_1^{u+} = Y_1^{d-} = Y_1^{d+} = \mathrm{I}_3 \tag{5}$$

### 4.2.2 System with a stand-by policy

Let us consider a further step in optimization of MT energy use: to switch off the machine when there is no demand for parts, i.e., when the buffer fills up. To evaluate effect of such a policy, a system model is necessary, and here we can exploit the properties of GTM which allow us to implement controlled on-threshold state transitions. The following management policy is defined: the upstream MT produces continuously to fill up the interoperational buffer (as it is nominally faster than the downstream machine) and when the buffer is full, it immediately goes into low-energy standby mode - in this case we consider a complete switch-off. The buffer level gradually decreases, as the demand of the downstream machine drains the stored inventory. The upstream MT wakes up when the buffer level falls below a settable threshold $x_{set}$. After wake-up it performs a warm-up cycle to reach the thermal stability, required assure workpiece quality, and resumes processing, again filling up the buffer. Similarly to the previous case, when producing, both machines can go down or to setup state and recover from it with defined transition rates. Applying the *GTM* approach, two buffer ranges, with a central threshold $x_{set}$ and a total size $b$, are defined:

$$X_1 = [0, x_{set}]$$
$$X_2 = [x_{set}, b] \quad (6)$$

The upstream machine has 2 additional states: stand-by $SB$ and warm-up $WU$, that can occur only in one of the two ranges. The downstream machine state behaves identically to the *no stand-by* policy case.

$$S_1^u = [UP, DN, SU, WU] \qquad \mathrm{S}_1^{\dagger}\ for\ x < x_{set}$$
$$S_2^u = [UP, DN, SU, SB] \qquad \mathrm{S}_2^{\dagger}\ for\ x > x_{set} \quad (7)$$
$$S_1^d = S_2^d = [UP, DN, SU]$$

Matrices containing transition rates are different: the machine breaks down or goes to setup in the same manner as before, but in the lower buffer range appears a new transition, when the machine transit from $WU$ to operational $UP$.

$$Q_1^{*\,u} = \begin{bmatrix} 0 & \lambda_{dn,u} & \lambda_{ch,u} & 0 \\ \lambda_{up,u} & 0 & 0 & 0 \\ \lambda_{su,u} & 0 & 0 & 0 \\ \lambda_{wu,u} & 0 & 0 & 0 \end{bmatrix}$$
$$Q_2^{*\,u} = \begin{bmatrix} 0 & \lambda_{dn,u} & \lambda_{ch,u} & 0 \\ \lambda_{up,u} & 0 & 0 & 0 \\ \lambda_{su,u} & 0 & 0 & 0 \\ 0 & 0 & 0 & 0 \end{bmatrix} \quad (8)$$

When buffer level goes under $x_{set}$, the $UP, DN, SU$ states remain the same and the $SB$ switches to $WU$. Because they are both the 4th states in both ranges, an identity matrix $I_4$ can represent this mapping. No state change occurs when the buffer is depleted. On the contrary, when the buffer full threshold $b$ is hit, the control policy immediately switches the upstream machine from $UP$ state to $SB$ ($Y_2^+$). In this way, the MT never blocks and does not waste energy while waiting for a free slot in the buffer.

$$Z_1^{u-} = Z_2^{u+} = [1\ 1\ 1\ 1] \quad (9)$$

$$Z_1^{u+} = Z_2^{u-} = [0\ 0\ 0\ 0]$$

$$Y_1^{u-} = Y_1^{u+} = Y_2^{u-} = I_4$$

$$Y_2^{u+} = \begin{bmatrix} 0 & 0 & 0 & 1 \\ 0 & 1 & 0 & 0 \\ 0 & 0 & 1 & 0 \\ 0 & 0 & 0 & 1 \end{bmatrix}$$

Implementation of the downstream machine is going to be very similar as in the previous case. $Q$ and $Y$ matrices remain the same for both ranges and the only difference is in $Z$ vectors which simply need to allow crossing of the central boundary:

$$\begin{aligned} Q_1^{*\,d} &= Q_2^{*\,d} \\ Y_1^{d-} = Y_1^{d+} &= Y_2^{d-} = Y_2^{d+} \\ Z_1^{u-} = Z_2^{u+} &= [1\ 1\ 1\ 1] \\ Z_1^{u+} = Z_2^{u-} &= [0\ 0\ 0\ 0] \end{aligned} \tag{10}$$

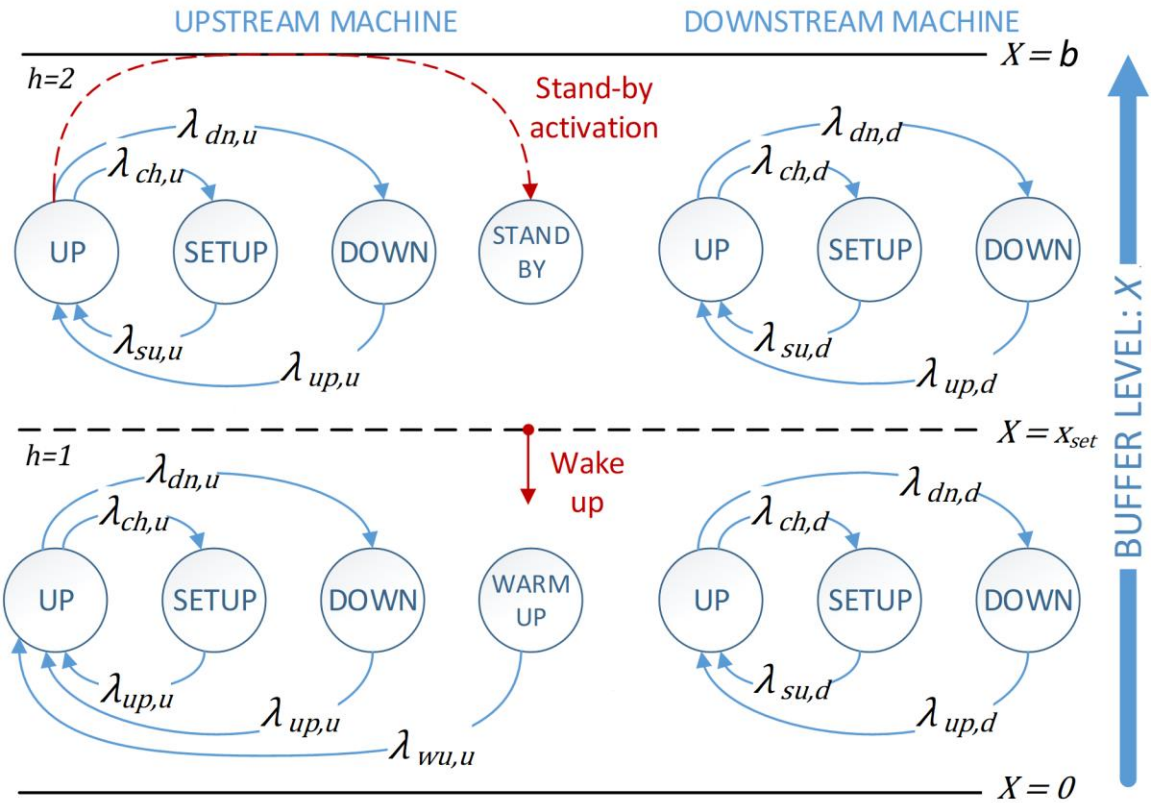


Fig. 4. GTM model diagram for a system with intermittent production realized through stand-by policy.

## 4.3 Per state energy demand estimation

Solving a GTM model of a system yields the steady-state probability of each state. Then one can compute throughput and average inventory retained in the buffer (Tolio and Ratti, 2018). Estimating mean energy-per-part for a certain work-point of the machine, i.e. a specific point from the machine Pareto MET, requires further computation. The power demand in UP state is given by Eq. (10 while, for remaining, non-productive, states is constant and known. Let us find all joint system states in which the upstream machine is in state $i$, i.e. on the threshold $(A_{i,h})$, or in the interior $(B_{i,h})$ of buffer range $h$:

$$A_{i,h} = \{S_h^\dagger[k] = S_h^u[i]S_h^d[*]: S_h^\dagger[k] \in \Theta_\mathrm{h}\}$$
$$B_{i,h} = \{S_h^\dagger[k] = S_h^u[i]S_h^d[*]: S_h^\dagger[k] \in \Upsilon_\mathrm{h} \cup \Delta_\mathrm{h} \cup \Phi_\mathrm{h}\} \quad (11)$$

Where $'*'$ denotes any state. Then, total probability of upstream machine being in state $i$ is given as sum of on-threshold and internal probability:

$$\pi_\mathrm{i} = \sum_\mathrm{h}^\mathrm{H} \sum_{S_h^\dagger[k] \in A_{i,h}} \pi(A_{i,h}) + \sum_\mathrm{h}^\mathrm{H} \sum_{S_h^\dagger[k] \in B_{i,h}} \mathrm{F}(B_{i,h}) \quad (12)$$

Knowing that machine average power demand in state $i$ is equal to $P_i$, average power consumption of the upstream machine is a sum of power and probability products:

$$\bar{P} = \sum_i^N P_i \, \pi_\mathrm{i} \quad (13)$$

An analogous approach is used to calculate downstream machine average power demand. The corresponding *mean energy per part* is defined as average power divided by average throughput of the system $Th$ :

$$\bar{E}_{part} = \frac{\bar{P}}{Th} \quad (14)$$

## 4.4 Manufacturing cost components

Costs are a fundamental driver in manufacturing systems setup. Whereas the energy bill may constitute a considerable portion of the overall cost $c$, it is relevant to understand how the considered policies affect production profitability as a whole. The considered cost components are: mean energy cost per part ($c_e$), inventory stored in the buffer ($c_i$), tooling cost ($c_t$), operator cost ($c_o$) and throughput loss cost ($c_{th}$). Whereas there are many ways to evaluate the throughput cost/profit, here the following assumption is used: if the estimated throughput $\overline{Th}$ is less than the nominal $Th_{nom}$ (referring to the no-policy case and to the reference processing rate of the non-optimized cycle), a penalty is received. The cost is considered to be 10% of the production added value per non-produced part. The formulas to compute the cost components are:

$$c_o = \frac{w_o}{\overline{Th}}$$

$$c_e = e_{price} \cdot E_{part}$$

$$c_{th} = \frac{max\left(0, Th_{nom} - \overline{Th}\right) \cdot 0.10 \cdot p_{price}}{\overline{Th}} \tag{15}$$

$$c_i = \frac{i_{price} \cdot \bar{x}}{\overline{Th}}$$

$$c_t = \sum_{i=1}^{n_{tool}} \frac{t_{i,time} \cdot t_{i,price}}{t_{i,life}}$$

It is important to note that only variable costs components were included in the objective function, instead than the total cost per part, to compare,, in relative terms, different strategies:

$$c = c_o + c_e + c_{th} + c_i + c_t \tag{16}$$

Tool life estimation is performed only if, for a specific workpiece geometrical feature, varying cutting parameters are used, to modify processing rate along the MET. The MET representation includes this

parameters information in the machine level hierarchical tree (Wójcicki et al., 2018a). The tooling cost of features is calculated, as a function of the processing rate, using Taylor's formula:

$$v \cdot {t_{life}}^{n} = C \tag{17}$$

Weighing the projected energy consumption against other key performance indicators and cost components, the system designer has wider perspective on how to optimize together energy consumption and other objective functions.

# 5 A transfer machine case study

To evaluate the proposed methodology, actual production data were used: a synthetically generated dataset could lead to distorted results and conclusions, far from industrial practice and needs. A section of a plant producing gas and liquid valves was surveyed, analysed and modelled. The model is composed of an upstream, three-station transfer MT (machining inlets into a valve cast) and a downstream assembly machine, as depicted in Fig. 5. The assumption that the system can never be starved or blocked by the unmodelled plant section is realistic, due to the large raw/completed part warehouse located on-site. The steady state performance of the system is evaluated under two operating regimes: continuous production and intermittent production with the upstream MT equipped with a stand-by mode.

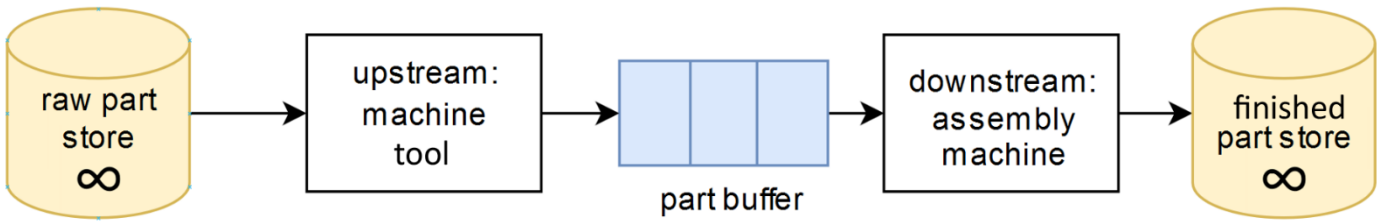


Fig. 5. Production cell layout

### 5.1.1 Information of production from plant records

The positive difference in the mean production rates of upstream and downstream machines (Table 1. System processing rates) allows realizing a stand-by control policy.

Table 1. System processing rates

| Name | Value |
|---|---|
| nom. Machining rate [p/h] | **60** |
| nom. assembly rate [p/h] | 52.3 |
| avg. prod rate [p/h] | 41.8 |

From an 88-day plant production log, failure and setup mean times were computed, whereas the mean warm-up time was measured directly (Table 2). The equivalent information on the assembly line reliability is reported in Table 3. State transition rates $\lambda_i$ used in the model are the inverse of a mean transition time: $\lambda_i = 1/MTTT_i$.

Table 2. Transfer machine (upstream) stop and recovery rate due to machine setup and failure, from plant log.

| **down time due to: FAILURE** | |
|---|---|
| Number of events [-] | 305.00 |
| MTTF [h] | 4.89 |
| MTTR [h] | 0.43 |
| **down time due to: SETUP** | |
| Number of events [-] | 42.00 |
| MTTF [h] | 35.53 |
| MTTR [h] | 2.29 |
| **Warm-up procedure** | |
| MTTR [h] | 0.25 |

Table 3. Stops and recovery rates for assembly line (downstream machine), from plant log

| Transitions | MTTR [h] | MTTF [h] |
|---|---|---|
| Assembly setup | 2.00 | 39.43 |
| Assembly down | 0.33 | 1.67 |

Exact information about manufacturing cost components were not disclosed by the manufacturer for confidentiality reasons, therefore approximate, but realistic, values were used for the case study (Table 4).

Fig. 6 presents tool life and tool contact time variations in function of the chosen cycle time, that are inputs to the cost function, for 2, out of 19, features of the work piece. The behavior is complex and is a result of machine level hierarchical optimization (Wójcicki et al., 2018a), considering multiple features spread across different processing stations of the machine, with variable cutting speed and feed.

Table 4. Coefficients used for cost estimation

| Name | Cost | Unit |
|---|---|---|
| Operator cost | 5 | €/hour/machine |
| Operation added value | 1 | €/part |
| Energy cost | 0.125 | €/kWh |
| Inventory cost | $1.2^{-5}$ | €/part/h |
| Buffer size cost | 0.2 | €/part/year |
| Tool life exponent $n$ | 0.115 | [-] |
| Machining constant $C$ | 210 | [-] |

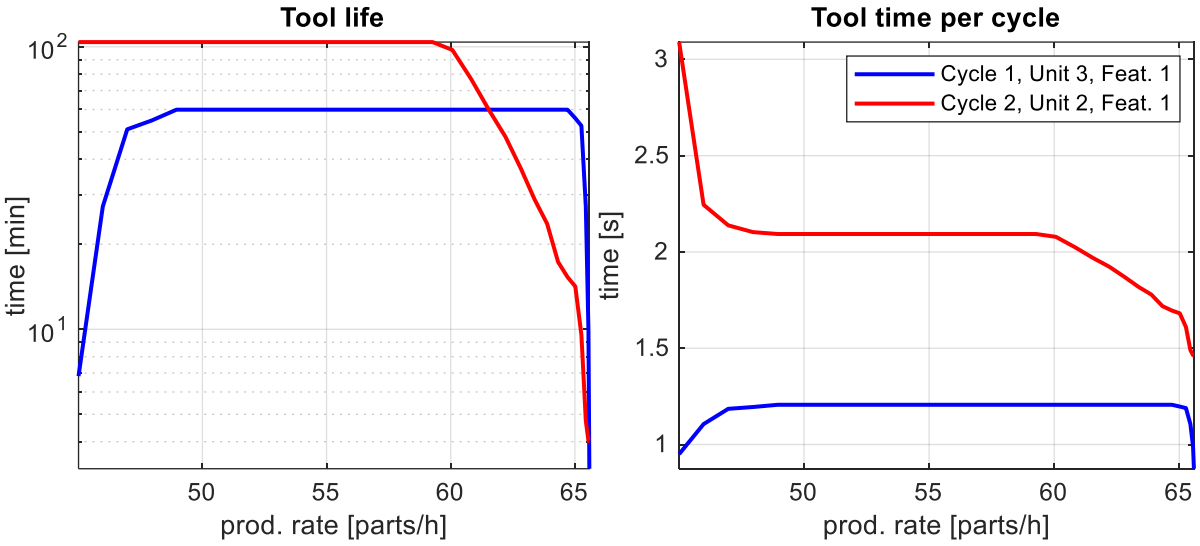


Fig. 6. Tool life and tool contact time for two selected geometrical features processed by the machine, obtained via MET.

### 5.1.2 State-dependent power use

The power used by the upstream MT depends on its operational state: their average power demand is listed in Table 5. The major difference is that the $UP$ state, which indicates processing, is described not by a constant value, as it is typically done, but by a function of the MT production rate, derived during the machine-level part of this study (Wójcicki et al., 2018a). Since *GTM* requires a single value for processing rate, it cannot utilize a functional description directly. Therefore, the model is executed for a range of possible processing rates, sampling the machine level *MET.*

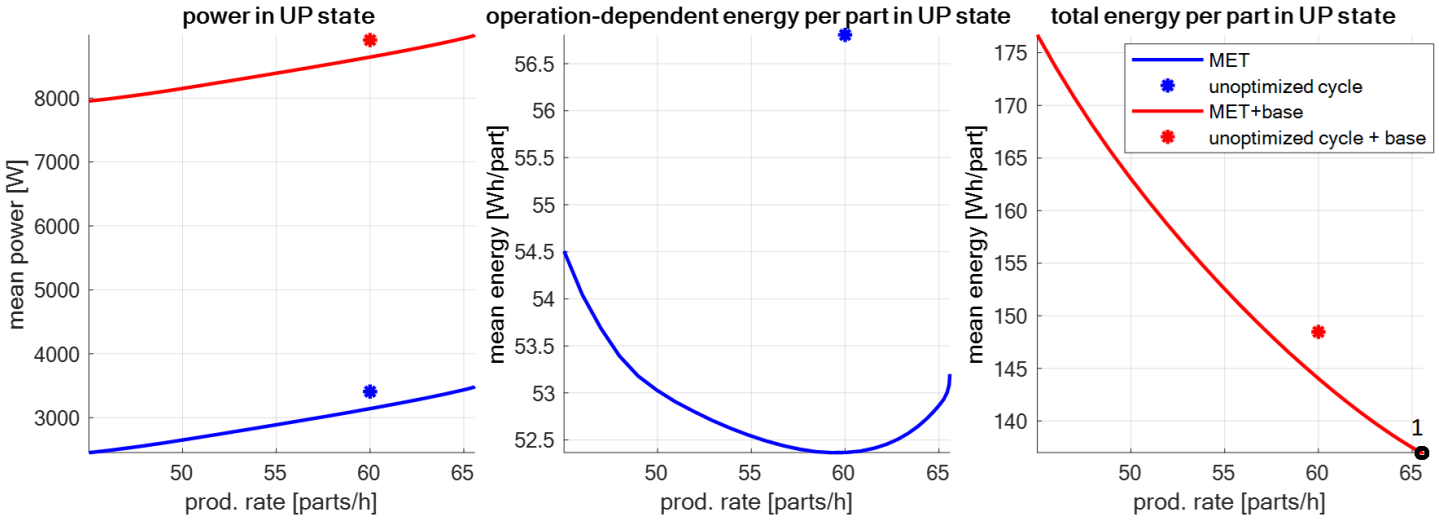


Fig. 7. Mean energy per part and mean processing power with and without base component a for MT in isolation. Point 1 indicates the optimal working point of the machine, with both minimal overall energy per part and fastest processing time.

As the tested machine does not have a low-power standby mode, $SB$ is assumed to be a complete shutdown of the machine, with zero power demand. Instead, setup and repair ($SU$ and $DN$) are performed while machine is on, as usual malfunctions, such as broken/worn tool replacement, part-loading robot jam, wrong work piece clamping or wrong program upload, are resolved without a complete shutdown. When the MT is blocked, it uses power associated to blocked state. This state is not distinguished in GTM, because, when the buffer is full, the machine will remain in the $UP$ state, however producing at a speed lower than the nominal (as GTM relies on a continuous part flow approximation). The equivalent percentage of time with blocked upstream machine is:

$$\mathscr{p}_{blocked} = 1 - \bar{\mu}(UP|x = b)/\mu_{nom} \quad (1)$$

Machine warm-up ($WU$) follows a routine: the machine starts, which takes 5 minutes with average power demand of 3kW, then a test part program without loaded material runs for 10 minutes and consumes average power of 10kW. In total, warm-up lasts for ¼ hour with 7.7kW mean power intake. All state powers are reported in (Table 5).

Table 5. Upstream MT states with associated mean power demand

| State | Power [kW] |
|---|---|
| $P_{up}$ | $P_{UP}(\mu)$ |
| $P_{base}$ | 5.5 |
| $P_{down}$ | 4.5 |
| $P_{blocked}$ | 4.5 |

| | |
|---|---|
| $P_{warm}$ | 7.7 |
| $P_{standby}$ | 0.0 |
| $P_{setup}$ | 4.5 |

# 6 Results and discussion

The GTM model was solved numerically, following the algorithm from (Tolio and Ratti, 2018), for both policy variants, considering, in the MET, a range of possible processing speeds and three buffer sizes ($b = 300$, $b = 600$ and $b = 900$). Additionally, in the case with the stand-by policy, a range of buffer threshold values $x_{set}$ (from 0 to $b$) was explored. Energy consumption of the MT was estimated as prescribed in section 4.3. The nominal throughput $Th_{nom}$ for the unoptimized cycle, here used as a reference, is 41.87 parts/h.

## 6.1 System without a stand-by policy

The resulting probability of the upstream MT being down or in the setup state results nearly constant for the whole range of production rate (Fig. 8). Instead, time spent being blocked increases with production rate, to match the mean production speed of the downstream machine. Therefore, producing faster means filling up the buffer quicker and, essentially, staying blocked longer.

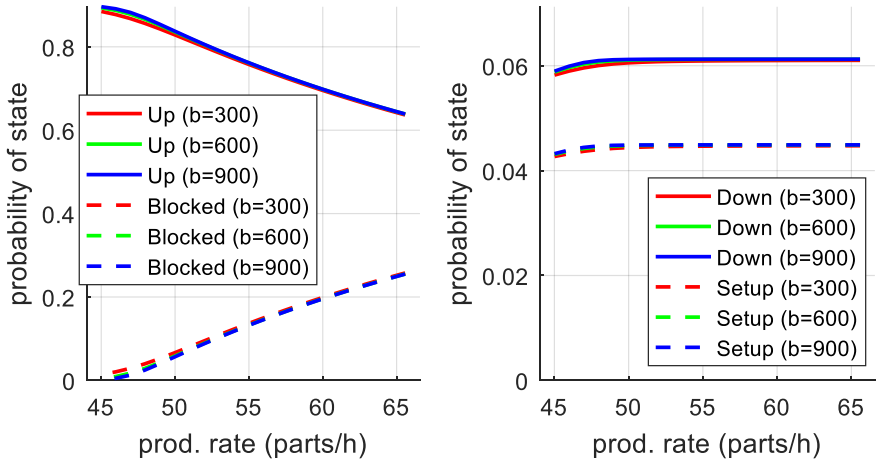


Fig. 8. MT state probability in function of its production rate. Three buffer sizes were considered.

State probability remains insensitive to buffer size however affects the mean throughput, which is reported in Fig. 9. Lower buffer size as well as lower processing speeds result in lower inventory, which increase the chance of the assembly starvation when the upstream MT fails.

The optimum from the energy consumption point of view is near the maximum processing rate of the MT, which is 65 parts/h, and only a negligible penalty at the top rate can be observed. The blocked machine wastes 4.5kW while the corresponding base component during production is 5.5kW. The difference of 1kW must be compared to the potential savings at the optimal rate depicted by the operation-dependent component of MET function (Fig. 7). Due to the optimization of the processing cycle suggested by MET, an increase in both processing rate and efficiency can be achieved comparing to the non-optimized machining cycle. A larger buffer allocation positively affects throughput, but also requires more inventory, with limited effect on the overall consumption per part.

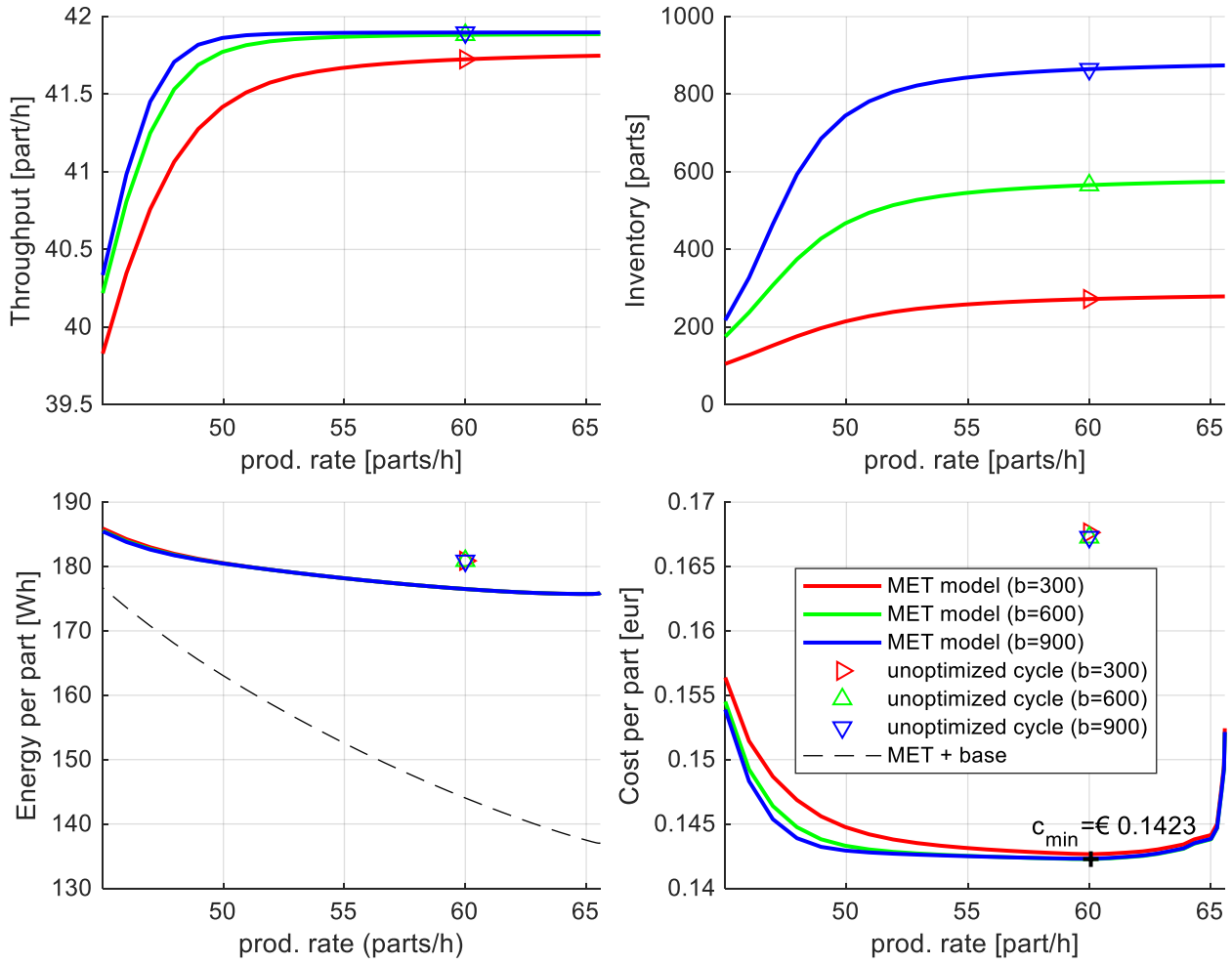


Fig. 9. System performance (throughput, mean inventory and energy per part).

The energy per part curve decreases slowly with increasing production rate, comparing to MET of MT in isolation. The difference can be explained by the fact that the blocked machine still demands a significant amount of power, as $P_{blocked}$ is only 1kW less than $P_{base}$: as a result, adopting the fastest machining cycle brings only marginal improvement in overall energy demand, giving an overall $E_{part}$ line relatively flat.

Considering that non-productive consumption of this particular machine, coming mainly from auxiliary sub-systems, could be significantly reduced by retrofitting them with their state-of-the-art energy-efficient counterparts (e.g. load sensing hydraulic unit, inverter-equipped chiller or passively cooled electrical cabinet), it is justified to evaluate potential effect of such changes. A hypothetical reduction of base consumption by one-third and two-thirds (Fig. 10) results in the energy consumption optimum shifting towards slightly lower processing rates: 1.9% and 6.2% less than maximum, respectively. A

sharper penalty for highest speed processing is now visible, as the operation-dependent portion of the power demand now has a comparatively higher impact on the overall consumption.

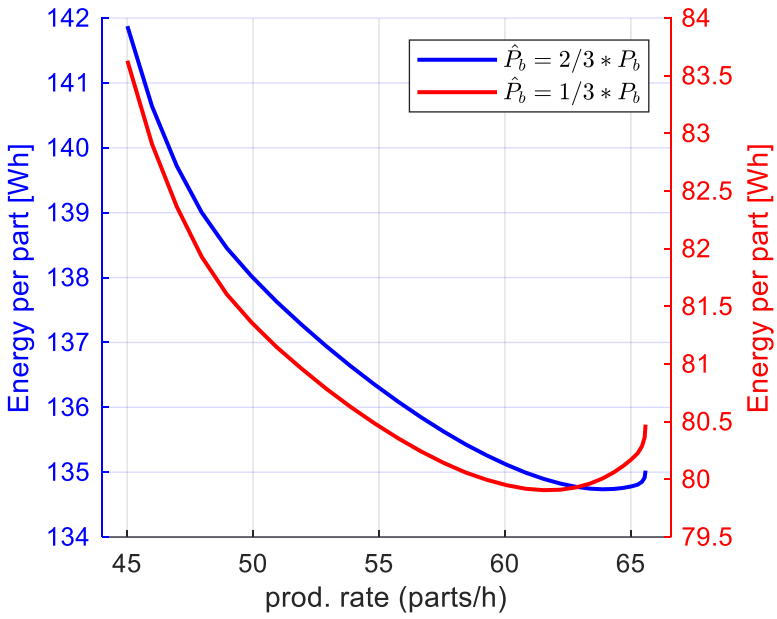


Fig. 10. System consumption with a hypothetical effect of energy efficient auxiliary subsystems retrofitting; $P_b$ reduced by 1/3 and 2/3, buffer size equal to 600.

## 6.2 System with stand-by policy (intermittent production)

This variant has an extra dimension: a control policy buffer threshold level, which triggers upstream MT stand-by. Fig. 11 shows that, in the dimension of processing rate, the MT behaviour is similar to the no-policy case. However, instead of being blocked, the machine turns into an energy-preserving stand-by. For low values of the threshold, the additional state, warm-up, is rarely occupied, as the downstream machine must deplete nearly all buffer content for the upstream machine to perform one stand-by/warm-up cycle. Raising the threshold value, MT spends an increasing amount of time in warm-up, especially if production rate is high.

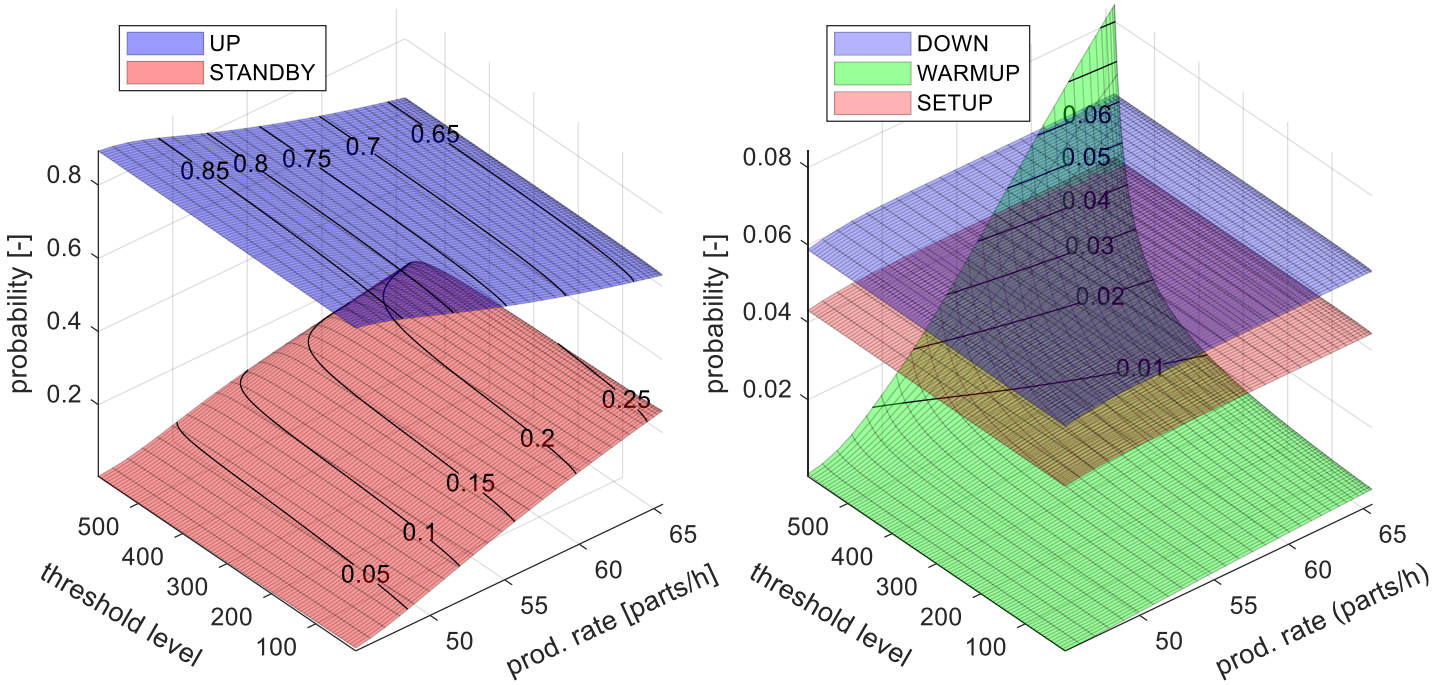


Fig. 11. Probability of states for GTM with stand-by policy. Buffer size b=600 was used.

Reducing threshold level increases the risk of assembly machine starvation: if buffer level is low and MT needs some time to warm up it may happen that the buffer will be completely emptied. This risk is even higher for unreliable machines. This can be seen well in Fig. 12: system throughput declines with decreasing threshold level and production, however, a certain threshold *plateau* can be observed for mid to high values of threshold and production rate.

As expected, the mean inventory is nearly proportional to threshold level and proportionally correlated with system throughput. If aiming at inventory reduction, it would be more efficient to act on changing threshold value or buffer size rather than the less impactful production rate.

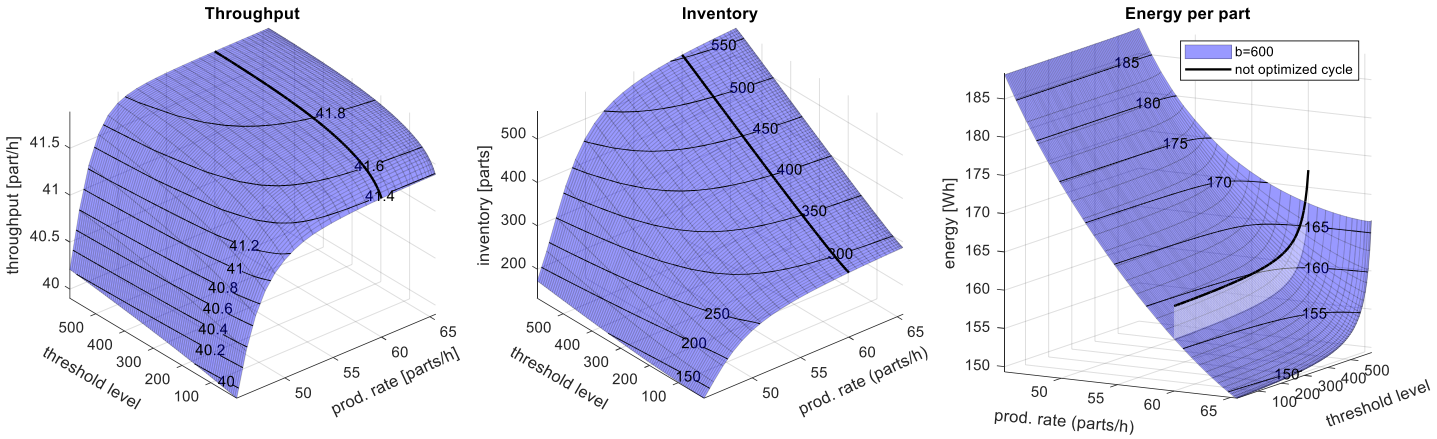


Fig. 12. Throughput (left) , average inventory (center) and energy per part (right) of the GTM model with stand-by in function of processing speed of MT and wake-up threshold level. Buffer size b=600 was used.

In terms of overall energy consumption per part, by hypothesis, there is no cost related to being in the stand-by state. Therefore, the optimum production rate must balance the increase of the operation-based energy with production rate against the total basal power of 5.5kW. For the analysed case study, the minimum (pt. 2 in Fig. 13) is very close to the highest production rate and lowest threshold. Going and returning from stand-by has a cost related to machine warm-up, both in terms of time and energy. The “price” to be paid depends on how often the machine goes into low energy mode because of the selected threshold level and, to a lesser degree, the overall buffer size. By comparing with the no-policy scenario, cost of machine non-productive state shifted from the production rate dimension to the threshold level dimension. Energy per part reduction reaches around 3-7% with respect to the reference machining cycle and around 7.5-15% comparing to the no-policy case (depending on the threshold level chosen).

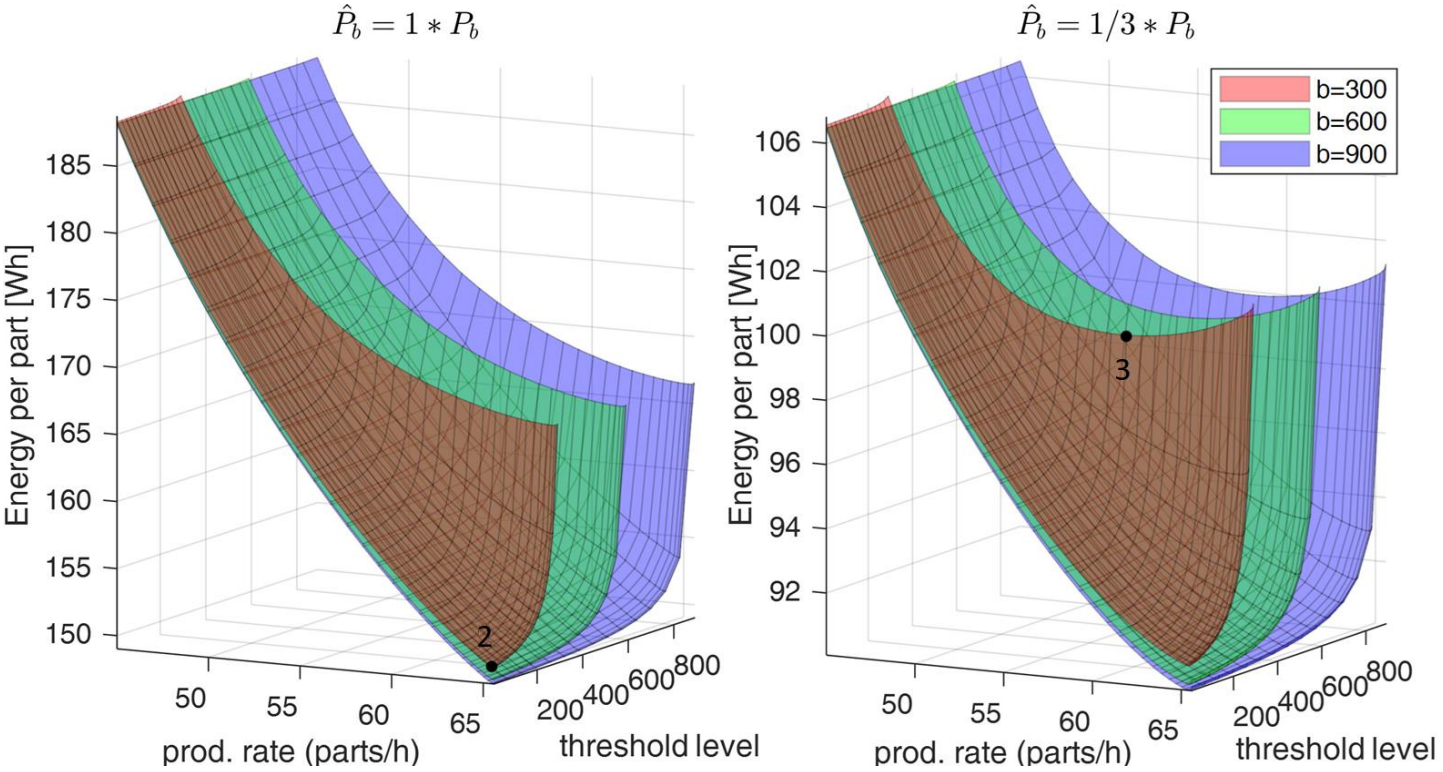


Fig. 13. Energy per part with stand-by policy for upstream MT. Left: nominal base consumption (minimum in Pt 2), right: base consumption reduced by 2/3 (minimum in Pt 3).

Like in the previous case, a potential two-third reduction of the base consumption was evaluated, (Fig. 13, right). The impact of this hypothetical reduction, aside from overall energy level, is visible mainly in the high threshold level range, for each buffer size: in this range the energy minimum point (pt. 3 in Fig. 13) shifts towards lower production rates. Such energy reduction strategy could be applied if maintaining the highest line throughput would be of primary concern. Moreover, there is a slight decrease (<1%) of overall energy demand with growing buffer size.

## 6.3 Machine tool cost analysis

The cost of operation was evaluated, for a system with stand-by policy, for the three buffers sizes (Fig. 14). Increasing buffer size pushes the optimal threshold to higher values: the machine spends less time and energy in the warm-up phase while reducing risk of downstream starvation. Even though the higher buffer size results in larger inventory, the overall balance is positive, and the cost is, marginally, reduced. A quick cost build-up can be observed on the right side of each cost surface: it is caused by steeply growing tool wear, if the machine operates close to an absolute performance limit.

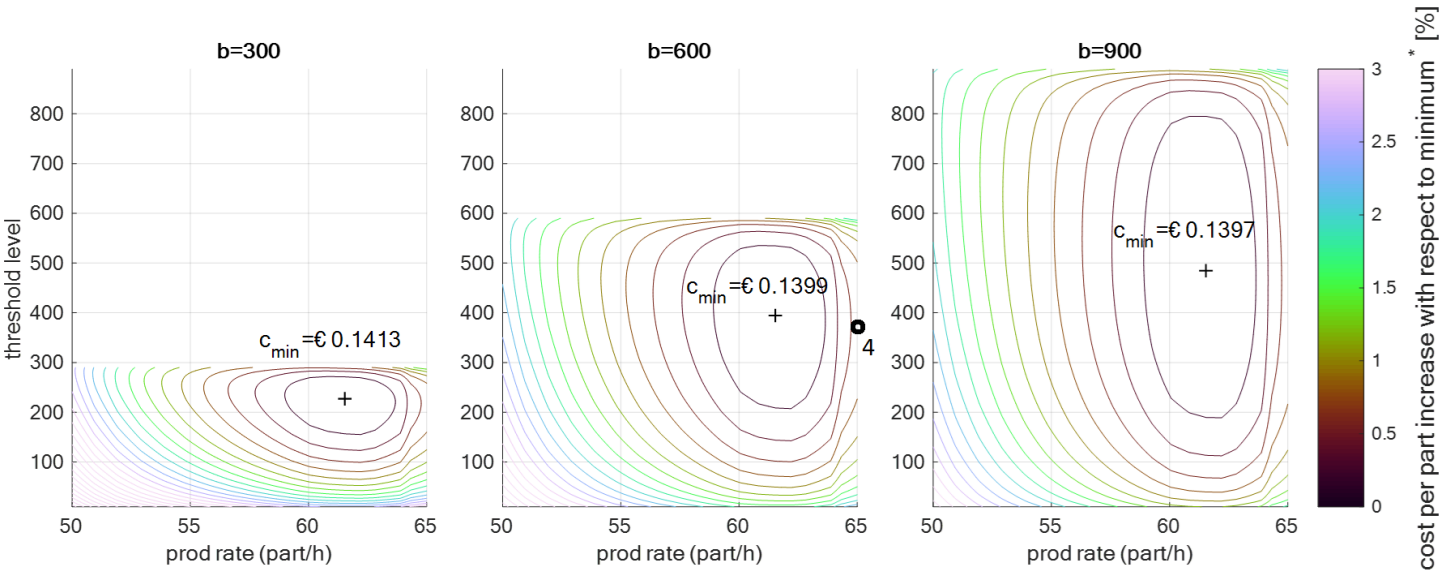


Fig. 14. Cost function for system with stand-by policy, for various buffer size. Coordinates of minimum (black cross) are annotated on each subplot. Pt. 4 indicates sub-optimal working point if MET and GTM models were applied sequentially, rather than jointly.

To better understand how energy consumption affects overall system optimum, a sensitivity analysis, changing machine basal power consumption (as in previous sub-sections) and energy price, has been performed (Fig. 15). In this scenario, energy price was doubled and tripled, which is not a probable evolution of the real energy market in the short term. However, this depicts a hypothetical impact of energy cost component on the entire system and could be manifested through financial incentives, promoting energy savings, or legislative actions such as carbon tax or further restrictions to EU Emissions Trading System (Fuss et al., 2018).

Decreasing the base consumption means emphasizing contribution of operation-based energy, which has a minimum value at lower processing rates (around 58-59 parts/h). Indeed, system optimum shifted towards this value, at the same time increasing the optimal threshold value, as less energy is lost in warm-up. On the contrary, increasing energy price generally pushes towards faster production (at expense of tool cost) and towards lower level of threshold, to reduce costly warm-up cycles. The cost of system operation becomes less sensitive to processing rate of the upstream machine when the its base power is reduced, as the energy demand response surface becomes flatter.

To further evaluate the impact of the proposed optimization strategy, that couples machine and system levels, the traditional approach, where machine level and system level problems are considered independently and solved sequentially, has been applied to the case with buffer size b=600. The result is represented by Pt. 4 in Fig. 14: the optimizer “pushes” the machine to work at the highest possible rate, as no information on the surrounding manufacturing system is taken into account. As a result, the machine tool ends up in the region of high tool wear, which is sub-optimal from the point of view of the overall cost. A joint cross-level optimization, instead, considering requirements, reliability and performance of the whole system, suggests the adoption of less intensive strategies, when required, and deliver a better performance at system level.

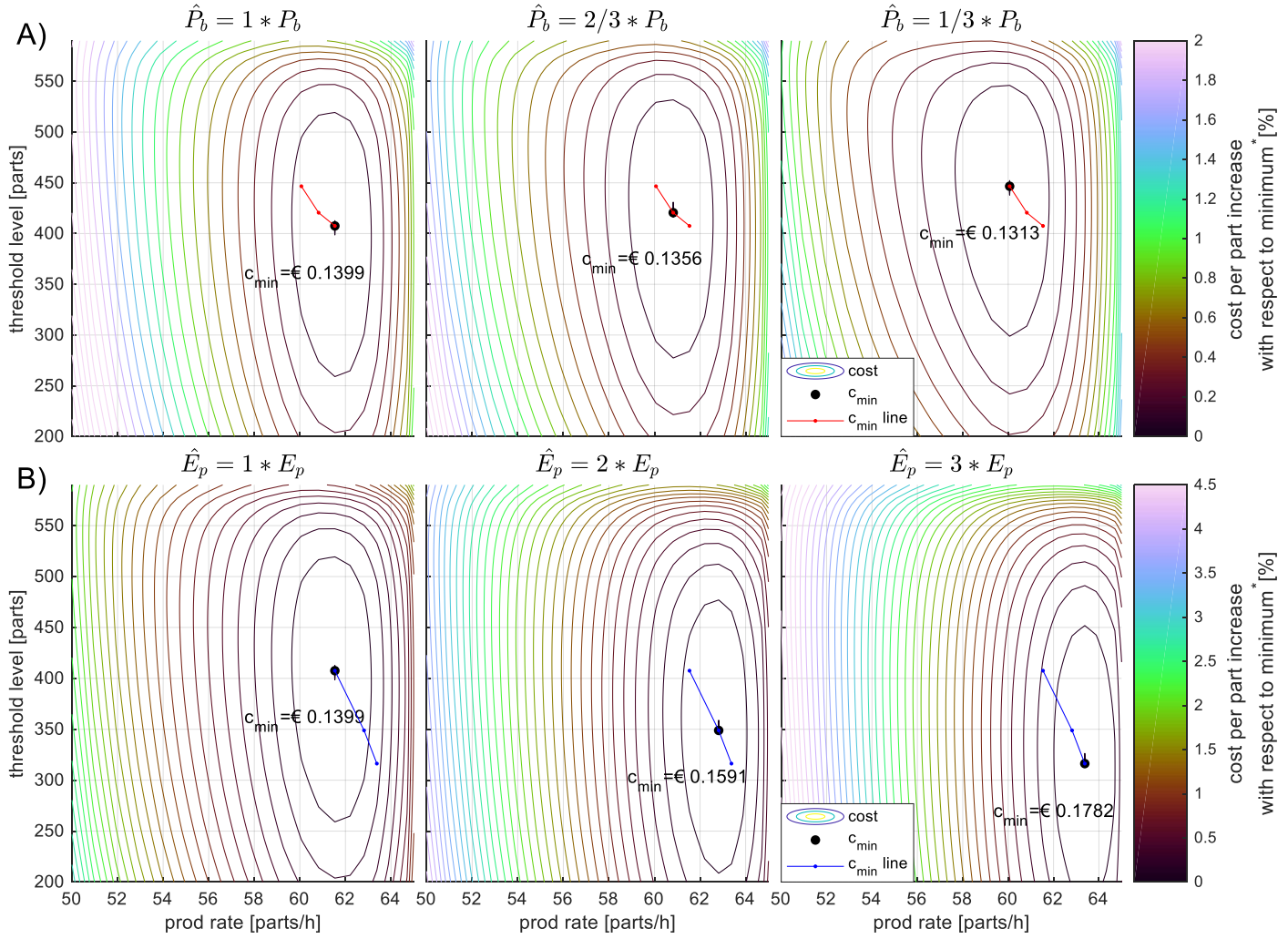


Fig. 15. Cost analysis for various, hypothetical values of base power $P_b$ (subplot A) and energy price $E_p$ (subplots B). Lines along which the system minimum moves are marked in red and blue, for $P_b$ and $E_p$ variations, respectively. Used buffer size $b = 600$. The percentual cost increase is normalized with respect to the minimum of each case to allow qualitative comparison between the cases.

The optimized machining cycle (Wójcicki et al., 2018a), applied to the system model without a policy, brought a noticeable reduction of cost per part and a modest energy saving (Table 6). It is because the reduction of energy consumption at process-level is focused only on the operation-dependent consumption, which makes a small portion of the whole consumption for the considered MT. On the other hand, the goal of improving efficiency is strongly correlated with improvement of tool life (Bhushan, 2013), which, in turn, reduces tooling costs, which is a significant portion of the overall cost. The optimum processing rate of the MT was slightly less compared to the reference case.

Adding a stand-by policy, the cost additionally has decreased, but by a small factor, whereas a nearly extra 13.5% energy reduction was observed. The strong effect of energy-saving policy is not visible in the overall cost so well, because, as the risk of downstream starvation increases, machine production rate must be higher to compensate for possible throughput loss. This partially negates savings obtained both on energy and inventory with higher tooling and operator costs.

Table 6. Summary of the savings on energy and cost for considered strategies

| Case | Upstream prod. rate [parts/h] | Cost per part [€] | Cost per part change [%] | Energy per part [Wh] | Energy per part change [%] |
|---|---|---|---|---|---|
| *Reference cycle, no system policy* | 60.12 | 0.2125 | --- | 180.9 | --- |
| *Cycle optimized at MT level, no system policy* | 60.05 | 0.1423 | −33.0 | 176.7 | −2.3% |
| *Cycle optimized at MT level, stand-by system policy* | 61.54 | 0.1399 | −34.2 | 154.9 | −14.8% |

# 7 Conclusions

The energy model of a machine tool in the context of a manufacturing system has been developed and analysed. The analysis exploits a *Minimum Energy-Time* (MET) function, which links a machine-level, high-resolution model, with a variable power and processing rate, to a system-level state model, which takes into account demand variability, random-failures and energy saving policies. A generalized threshold model has been developed to analyse buffer sizing and threshold level setting in a real industrial manufacturing system. Strategies for energy reduction have been tested, also considering other important performance indicators i.e. throughput loss, tooling and inventory cost. Using MET function to represent MT processing allowed not only to correlate energy and processing capabilities of the machine but also gave insight into low level phenomena, such as tool life variation with processing speed.

Obtained results showed that the problem of MT cost optimization is not trivial: the optimum is not located at any boundary. In practice, a significant improvement in energy consumption can be achieved using a low energy stand-by state. The case study demonstrated that increasing buffer size (which can be considered against lean production guidelines) has limited but positive impact on system

performance, including energy demand. Optimal work-point is located in the area of high processing speed and mid-to-high stand-by threshold level, in the throughput “plateau”. In this range, the optimum position will change depending on several factors: energy, inventory and tool life. Analysis revealed that lowering machine base consumption allows producing parts more slowly and with a higher safety margin: high threshold decreases risk of downstream starvation. Increasing purely energy cost acts inversely, forcing higher processing rate and lower threshold to reduce costly warm-up cycles. The system global cost minimum was found: implementing a stand-by policy with a production rate of 61.5 parts/h and the threshold level of around 2/3 of the buffer size which resulted in reduction of the energy demand by 14.8% and cost by 34.2% comparing to the MT reference cycle.

If the MT is optimized in isolation, only on MET without using the system model, the resulting operating point would be one of the nadir points of the cycle-time/energy Pareto front, as no other criteria would be available. For the case of this particular machine, due to very high base power component, both these points are in fact the same point (pt. 1, Fig. 7) corresponding to a processing rate of 65 part/s hour, around 3.5 parts/hour faster than the actual optimum. Considering this locally optimized process in the GTM for a subsequent system optimization would lead to the adoption of a sub-optimal policy (pt. 4, Fig. 14), as one design variable (processing rate) is constraint upfront. Concluding, optimizing system using MET and GTM independently, in sequence, is inherently sub-optimal and leads to increased operation cost of the system. Performing joint optimization allows for an optimal setup of a machine, as it considers both machine-specific and system-specific objective functions to be minimized simultaneously.

The presented methodology can be used to evaluate performance of discrete manufacturing system both a-priori (during design or configuration) and a-posteriori (after deployment). In the former case it could support selecting various candidate machines or machine subsystems, whereas, in the latter, fine-tuning of the processing cycle in a given system context or a what-if analysis, considering MT component replacement to improve energy and/or cost performance.

## Acknowledgements

The authors gratefully acknowledge the European Commission, for its support of the Marie Curie program through the ITN EMVeM project [Grant agreement 315967], and the Italian Ministry of Economic Development, for its support via the Accordo di Programma CNR-MSE PT 2015, Gruppo Tematico D.3: Processi e macchinari industriali.

## References

Bhushan, R.K., 2013. Optimization of cutting parameters for minimizing power consumption and maximizing tool life during machining of Al alloy SiC particle composites. J. Clean. Prod. 39, 242–254. https://doi.org/10.1016/J.JCLEPRO.2012.08.008

Chang, Q., Xiao, G., Biller, S., Li, L., 2013. Energy Saving Opportunity Analysis of Automotive Serial Production Systems (March 2012). IEEE Trans. Autom. Sci. Eng. 10, 334–342. https://doi.org/10.1109/TASE.2012.2210874

Chou, Y.-L., Yang, J.-M., Wu, C.-H., 2020. An energy-aware scheduling algorithm under maximum power consumption constraints. J. Manuf. Syst. 57, 182–197. https://doi.org/10.1016/j.jmsy.2020.09.004

Colledani, M., Tolio, T., 2005. IMPACT OF STATISTICAL PROCESS CONTROL ( SPC ) ON THE PERFORMANCE OF PRODUCTION SYSTEMS-Part Two ( large systems ).

Demir, L., Tunali, S., Eliiyi, D.T., 2014. The state of the art on buffer allocation problem: a comprehensive survey. J. Intell. Manuf. 25, 371–392. https://doi.org/10.1007/s10845-012-0687-9

Diaz C., J.L., Ocampo-Martinez, C., 2019. Energy efficiency in discrete-manufacturing systems: Insights, trends, and control strategies. J. Manuf. Syst. 52, 131–145. https://doi.org/10.1016/j.jmsy.2019.05.002

Diaz C., J.L., Ocampo-Martinez, C., Olaru, S., 2020. Dual mode control strategy for the energy efficiency of complex and flexible manufacturing systems. J. Manuf. Syst. 56, 104–116. https://doi.org/10.1016/j.jmsy.2020.05.009

Dietmair, A., Verl, A., 2009. A generic energy consumption model for decision making and energy efficiency optimisation in manufacturing. Int. J. Sustain. Eng. 2, 123–133. https://doi.org/10.1080/19397030902947041

Frigerio, N., Matta, A., 2014. Energy saving policies for a machine tool with warm-up, stochastic arrivals and buffer information, in: 2014 IEEE International Conference on Automation Science and Engineering (CASE). pp. 646–651. https://doi.org/10.1109/CoASE.2014.6899396

Frigerio, N., Matta, A., Ferrero, L., Rusinà, F., 2013. Modeling Energy States in Machine Tools: An Automata Based Approach, in: Re-Engineering Manufacturing for Sustainability. Springer Singapore, Singapore, pp. 203–208. https://doi.org/10.1007/978-981-4451-48-2_33

Fuss, S., Flachsland, C., Koch, N., Kornek, U., Knopf, B., Edenhofer, O., 2018. A Framework for Assessing the Performance of Cap-and-Trade Systems: Insights from the European Union

Emissions Trading System. Rev. Environ. Econ. Policy 12, 220–241. https://doi.org/10.1093/reep/rey010

Gebennini, E., Grassi, A., 2015. Discrete-time model for two-machine one-buffer transfer lines with buffer bypass and two capacity levels. IIE Trans. 47, 715–727. https://doi.org/10.1080/0740817X.2014.952849

Hu, L., Zheng, H., Shu, L., Jia, S., Cai, W., Xu, K., 2020. An investigation into the method of energy monitoring and reduction for machining systems. J. Manuf. Syst. 57, 390–399. https://doi.org/10.1016/j.jmsy.2020.10.012

Kant, G., Sangwan, K.S., 2015. Predictive Modelling for Energy Consumption in Machining Using Artificial Neural Network. Procedia CIRP 37, 205–210. https://doi.org/10.1016/J.PROCIR.2015.08.081

Levantesi, R., Matta, A., Tolio, T., 2003. Performance Evaluation of Continuous Production Lines with Machines Having Different Processing Times and Multiple Failure Modes. Perform Eval 51, 247–268. https://doi.org/10.1016/S0166-5316(02)00098-6

Mawson, V.J., Hughes, B.R., 2019. The development of modelling tools to improve energy efficiency in manufacturing processes and systems. J. Manuf. Syst. 51, 95–105. https://doi.org/10.1016/j.jmsy.2019.04.008

Mouzon, G., Yildirim, M.B., Twomey, J., 2007. Operational methods for minimization of energy consumption of manufacturing equipment. Int. J. Prod. Res. 45, 4247–4271. https://doi.org/10.1080/00207540701450013

Peng, T., Xu, X., 2014. Energy-efficient machining systems: a critical review. Int. J. Adv. Manuf. Technol. 72, 1389–1406. https://doi.org/10.1007/s00170-014-5756-0

Peng, T., Xu, X., 2013. A Universal Hybrid Energy Consumption Model for CNC Machining Systems, in: Re-Engineering Manufacturing for Sustainability. Springer Singapore, Singapore, pp. 251–256. https://doi.org/10.1007/978-981-4451-48-2_41

Peng, T., Xu, X., Wang, L., 2014. A novel energy demand modelling approach for CNC machining based on function blocks. J. Manuf. Syst. 33, 196–208. https://doi.org/10.1016/j.jmsy.2013.12.004

Prabhu, V. V., Jeon, H.W., Taisch, M., 2013. Simulation Modelling of Energy Dynamics in Discrete Manufacturing Systems. Springer, Berlin, Heidelberg, pp. 293–311. https://doi.org/10.1007/978-3-642-35852-4_19

Prabhu, V. V., Jeon, H.W., Taisch, M., 2012. Modeling green factory physics — An analytical approach, in: 2012 IEEE International Conference on Automation Science and Engineering (CASE). IEEE, pp. 46–51. https://doi.org/10.1109/CoASE.2012.6386361

Rief, M., Karpuschewski, B., Kalhöfer, E., 2017. Evaluation and modeling of the energy demand during machining. CIRP J. Manuf. Sci. Technol. 19, 62–71. https://doi.org/10.1016/j.cirpj.2017.05.003

Tolio, T., Ratti, A., 2013a. Performance evaluation of two-machines line with generalized thresholds, in: Proceedings of the 9 Th International Conference on Stochastic Models of Manufacturing and Service Operations. Seeon, Germany, pp. 221–229.

Tolio, T., Ratti, A., 2013b. Performance evaluation of two-machines line with generalized thresholds, in: Proceedings of the 9 Th International Conference on Stochastic Models of Manufacturing and Service Operations. Seeon, Germany, pp. 221–229.

Tolio, T.A.M., Ratti, A., 2018. Performance evaluation of two-machine lines with generalized thresholds. Int. J. Prod. Res. 56, 926–949. https://doi.org/10.1080/00207543.2017.1420922

Verl, A., Westkämper, E., Abele, E., Dietmair, A., Schlechtendahl, J., Friedrich, J., Haag, H., Schrems, S., 2011. Architecture for Multilevel Monitoring and Control of Energy Consumption, in: Glocalized Solutions for Sustainability in Manufacturing. Springer Berlin Heidelberg, Berlin, Heidelberg, pp. 347–352. https://doi.org/10.1007/978-3-642-19692-8_60

Wang, J., Li, S., Liu, J., 2013. A Multi-Granularity Model for Energy Consumption Simulation and Control of Discrete Manufacturing System, in: Qi, E., Shen, J., Dou, R. (Eds.), The 19th International Conference on Industrial Engineering and Engineering Management. Springer Berlin Heidelberg, pp. 1055–1064.

Weinert, N., Mose, C., 2014. Investigation of Advanced Energy Saving Stand by Strategies for Production Systems. Procedia CIRP 15, 90–95. https://doi.org/10.1016/J.PROCIR.2014.06.009

Wójcicki, J., 2017. Energy efficiency of machine tools. Politecnico di Milano. https://doi.org/10.13140/RG.2.2.30523.11047

Wójcicki, J., Bianchi, G., 2015. MINIMIZATION OF ENERGY CONSUMPTION OF A MACHINE TOOL : A MULTI-LEVEL APPROACH, in: 23rd ABCM International Congress of Mechanical Engineering. https://doi.org/10.20906/CPS/COB-2015-2719

Wójcicki, J., Bianchi, G., Tolio, T., 2018a. Hierarchical modelling framework for machine tool energy optimization. J. Clean. Prod. 204, 1044–1059. https://doi.org/10.1016/J.JCLEPRO.2018.09.030

Wójcicki, J., Leonesio, M., Bianchi, G., 2018b. Integrated energy analysis of cutting process and spindle subsystem in a turning machine. J. Clean. Prod. 170, 1459–1472. https://doi.org/10.1016/j.jclepro.2017.09.234

Zavanella, L., Zanoni, S., Ferretti, I., Mazzoldi, L., 2015. Energy demand in production systems: A Queuing Theory perspective. Int. J. Prod. Econ. 170, 393–400. https://doi.org/10.1016/J.IJPE.2015.06.019

Zhou, L., Li, Jianfeng, Li, F., Meng, Q., Li, Jing, Xu, X., 2016. Energy consumption model and energy efficiency of machine tools: a comprehensive literature review. J. Clean. Prod. 112, 3721–3734. https://doi.org/10.1016/J.JCLEPRO.2015.05.093

# Appendix A - Nomenclature

Symbols used in the paper are listed in Table A-1.

Table A-1. List of symbols

| Symbol | Description |
|---|---|
| $A_{i,h}$ | Set of all joint threshold states where upstream machine is in state $i$ |
| $B_{i,h}$ | Set of all joint non-threshold states where upstream machine is in state $i$ |
| $b$ | Buffer size |
| $c$ | Total cost per part |
| $c_e$ | Mean energy cost per part and |
| $c_i$ | Inventory stored in the buffer |
| $c_t$ | Tooling cost |
| $c_o$ | Operator cost |
| $c_{th}$ | Throughput loss cost |
| $\Delta_h$ | Partition of joint machine states where buffer level is rising |
| $e_{price}$ | Energy price |
| $\bar{E}_{part}$ | Mean energy per part |

| | |
|---|---|
| $\Phi_h$ | Partition of joint machine states where buffer level is not changing |
| $f(x, S_h)$ | Probability density function of |
| $F(S_h)$ | Total probability |
| $h$ | Buffer range index |
| $i_{price}$ | Price for storing inventory |
| $\lambda_{i,?}$ | State $i$ transition rate for a machine where ? stands for upstream (u) or downstream (d) machine |
| $MET(t)$ | Minimal operation-depended energy per part achievable given cycle time $t$ |
| $\mu$ | Nominal processing rate of a machine |
| $n, C$ | Taylor's formula coefficients related to material and tool |
| $P_i$ | Mean power in state $i$ |
| $\bar{P}$ | Mean power demand of the upstream machine |
| $P_{UP}(\mu)$ | Mean power of upstream machine in UP state given nominal processing rate |
| $p_{price}$ | Part price |
| $\pi(\Theta)$ | Probability of being in a threshold state |
| $\pi_i$ | Total probability of the upstream machine being in state $i$ |
| $t_{price}$ | Tool price |
| $t_{life}$ | Expected tool life |
| $t_{time}$ | Tool use time |
| $Th$ | Average system throughput |
| $Th_{nom}$ | Nominal throughput |
| $\Theta_h$ | Set of threshold states |
| $v(S)$ | Difference in nominal processing rate between the upstream and the downstream machine in state $S$ |
| $v$ | Cutting speed |
| $w_o$ | Operator wage |
| $x$ | Buffer level |
| $\bar{x}$ | Mean inventory |
| $x_h^-, x_h^+$ | Upper and lower buffer threshold limits |
| $x_{set}$ | Stand-by activation buffer level trigger |
| $X$ | Threshold range vector |
| $Y_h^-, Y_h^+$ | Probabilities of state transitions when hitting a threshold from top or bottom |
| $Z_h^-, Z_h^+$ | Probability of jumping to a threshold state from top of bottom |

# Appendix B - Generalized Threshold Model

This appendix, to allow reproducibility of the discussed analysis, describes the Generalized Threshold Model developed to analyse the industrial test case.

Markov-chain based GTM was firstly introduced in (Tolio and Ratti, 2013) and then generalized in (Tolio and Ratti, 2018). It allows creating a *building block* model using different state transition diagrams to

describe machine behaviour in various ranges of the buffer level (Fig. 16). Similarly, certain actions can be triggered upon hitting a threshold (a boundary between neighbouring ranges): this capability has been exploited in this work to implement an energy-saving policy. GTM approximates a discrete part flow with a continuous material flow; similarly, buffer level is also a continuous quantity. The thresholds denote ranges of buffer level in which upstream ($u$) and downstream ($d$) machine can assume different sets of states $S_h^u$ and $S_h^d$ and transition rates between them (therefore realizing different machine behaviour). The joint machine states matrix $\mathrm{S}_\mathrm{h}^\dagger$ is their Kronecker product:

$$\mathrm{S}_\mathrm{h}^\dagger = S_h^u \otimes S_h^d \tag{1}$$

The model assumes different nominal production rate in a state $i$ of range $h$ denoted as $\mu(S_h^u[i])$ and $\mu\left(S_h^d[i]\right)$.

Machines can jump from one state to another, defining the proper system dynamics, are given in form of matrices containing all the transition rates ${Q_h^*}^u$ and ${Q_h^*}^d$, being a sum of operation- and time-dependent transitions (Tolio and Ratti, 2018):

$$\begin{aligned} {Q_h^*}^u &= \hat{Q}_h^u + \overleftrightarrow{Q}_h^u \\ {Q_h^*}^d &= \hat{Q}_h^d + \overleftrightarrow{Q}_h^d \end{aligned} \tag{2}$$

Having defined $v$ as the difference in production rate of the upstream and the downstream machine, joint machine states $\mathrm{S}_\mathrm{h}^\dagger$, are partitioned in three groups:

$$\begin{aligned} \Upsilon_h &= \left[S_h^\dagger[k]: v\left(S_h^\dagger[k]\right) > 0\right] \\ \Delta_h &= \left[S_h^\dagger[k]: v\left(S_h^\dagger[k]\right) < 0\right] \\ \Phi_h &= \left[S_h^\dagger[k]: v\left(S_h^\dagger[k]\right) = 0\right] \end{aligned} \tag{3}$$

$\Upsilon$ set contains states in which upstream machine produces, nominally, faster than downstream, therefore buffer level is rising. Respectively, the $\Delta$ set contains states in which buffer level is falling and, lastly, in $\Phi$ buffer level remains constant (e.g. when both machines are down), see Fig. 16.

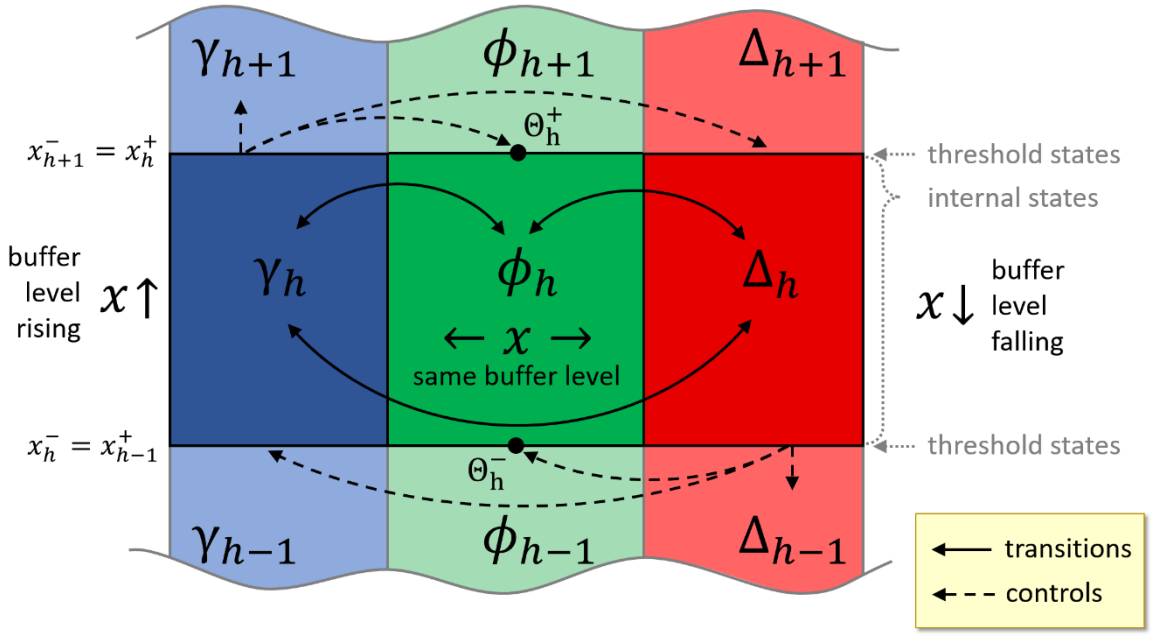


Fig. 16. Graphical representation of generalized threshold model at range $h$. The behavior of the system is shown for the internal states and on the threshold, along with the possible transitions and control actions.

To complete the formulation the around-threshold behaviour must be defined. Threshold $x_h^-$ or $x_h^+$ (Fig. 16) is reached when buffer level changes (states $\Upsilon_h$ or $\Delta_h$). In used notation " + " indicates that threshold is hit from the bottom (while buffer level was rising) and "– " from above (when buffer level is falling), in $\Upsilon$ or $\Delta$ states. When a threshold is hit, a number of events can occur: system can stay in one of the threshold states (belonging to $\Theta_h$), can transit from $\Upsilon_h$ to $\Delta_h$ or from $\Delta_h$ to $\Upsilon_h$, re-entering interior of buffer range from where it started, or pass through a threshold to the next range ($\Upsilon_h \rightarrow \Upsilon_{h+1}$ or $\Delta_h \rightarrow \Delta_{h+1}$).

The behaviour of a system while hitting a threshold is described in each range and for each machine independently using $Z_h^+$, $Z_h^-$, $Y_h^+$ and $Y_h^-$ matrices. $Y_h^+$ defines the mapping from states in range $h$ to $h+1$ on hitting a threshold. When threshold is hit from above an analogous matrix $Y_h^-$ is used. Values in the $Y_h$ matrices indicate the probability of state jump. $Z_h^+$ and $Z_h^-$ vectors indicate whether a given system threshold can ("0") or cannot ("1") be overcome. If, for a given machine state, a threshold is reached and for that state the $Z_h^+$ entry is 1, the production rate of the upstream is reduced to keep the system on that threshold.

Solving a GTM model computes the probability of joint-states when system is in steady state. It is defined as a probability of threshold states $\pi(\Theta_{\mathrm{h}})$ and probability density function (PDF) of buffer level x for system internal states:

$$f(x, S_h) = \begin{bmatrix} f(x, \Upsilon_{\mathrm{h}}) \\ f(x, \Delta_{\mathrm{h}}) \\ f(x, \Phi_{\mathrm{h}}) \end{bmatrix} \tag{4}$$

whereas total probability of a joint-state while in the interior is an integral of the PDF over the selected buffer range:

$$F(S_h) = \int_{x_h^-}^{x_h^+} f(x, S_h) dx \tag{5}$$